THE JOURNAL OF PHYSICAL CHEMISTRY C

Article

pubs.acs.org/JPCC

Noncovalent Approach toward the Construction of Nanofluidic Diodes with pH-Reversible Rectifying Properties: Insights from Theory and Experiment

Gonzalo Pérez-Mitta,*,† Alberto Albesa,† Facundo M. Gilles,† María Eugenia Toimil-Molares,‡ Christina Trautmann,‡,§ and Omar Azzaroni*,†

†Instituto de Investigaciones Fisicoquímicas Teóricas y Aplicadas (INIFTA), Departamento de Química, Facultad de Ciencias Exactas, Universidad Nacional de La Plata, CONICET-CC 16 Suc. 4, La Plata 1900, Argentina

‡GSI Helmholtz Centre for Heavy Ion Research GmbH, 64289 Darmstadt, Germany

§Technische Universität−Darmstadt, 64289 Darmstadt, Germany

Supporting Information

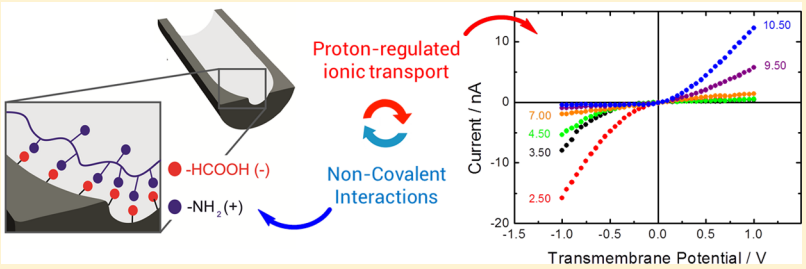

ABSTRACT: In this paper, the fabrication of a biomimetic nanofluidic diode whose ionic transport characteristics can be completely modulated with the proton concentration in solution is demonstrated. The fabrication procedure involves the electrostatic assembly of poly(allylamine hydrochloride) (PAH) into a track-etched conical nanochannel. A fully reversible, zwitterionic-like behavior with important implications for the supramolecular interactions of the PAH within confined spaces was observed. The experimental design constitutes a facile venue for the fabrication of functional nanofluidic devices and paves the way for a number of applications in nanofluidics and biosensing. Furthermore, in order to explain the experimental results and to obtain physicochemical information about the system, theoretical modeling using a continuous model based on Poisson−Nernst−Planck equations and a stochastic model using Monte Carlo simulations were performed. Good agreement between experiments and theory was found.

INTRODUCTION

Nanofluidics is an important emerging field within nanosciences that promises interesting applications in materials science, engineering, and biomedical research among other disciplines.[1−4,4] The unique transport properties of solid-state nanocannels, which resemble several functional features of biological channels, such as ion selectivity and ionic-gating, has sparked the interest of "nanoscientists" worldwide and has increased their willingness to use these nanoarchitectures as nanofluidic elements.[5−7]

Several approaches to the construction of artificial nanometric fluidic devices have been developed, from biological to fully abiotic designs,[8] each of them with particular advantages and disadvantages. Among the most common problems is the lack of mechanical stability exhibited by biological pores, and, in the case of artificial pores, the main issue is that the type of material that can be used strongly depends on the fabrication technique. For example, the focused ion beam technique demands that the thickness of the substrate that would contain the nanopore does not exceed few hundreds of nanometers.[9]

In this regard, the track-etching method emerges as one of the most interesting procedures for obtaining abiotic nanochannels. The main advantage of this technique is its flexibility to tailor the geometry and size of the nanochannels. Furthermore, this technique can be adapted to a wide variety of materials. The procedure consists, first, of the irradiation of a dielectric foil with swift heavy ions. The ion tracks created by the ions are subsequently dissolved by chemical etching. Appropriate etching conditions are chosen depending on the template material. Thus, for example, for typical condensation polymers such as polycarbonate or polyethylene terephthalate, the etching procedure consists of an alkaline hydrolysis using highly concentrated alkali solutions. Ultimately, this procedure allows the reproducible fabrication of nanoscale channels,[10] with tailored geometry (e.g., conical, cylindrical, biconical) and controlled diameter (>10 nm).

Received: February 20, 2017
Revised: April 3, 2017
Published: April 5, 2017

DOI: 10.1021/acs.jpcc.7b01639
J. Phys. Chem. C 2017, 121, 9070−9076

The possibility of regulating the nanochannel geometry is of paramount importance because a longitudinal asymmetry in the geometry of a nanochannel yields an asymmetric ionic conductance that produces a diode-like, non-ohmic behavior, i.e., rectification in the ionic current.[11,12] In addition, it has been shown that the rectification of ionic currents through nanochannels stems from changes in the selective transport of ions and, consequently, has a strong dependence on the surface charge of the channels, both in sign and magnitude. Therefore, in order to regulate the rectification of a nanochannel and the selective transport of ionic species it is necessary to regulate the surface charge of the nanochannel in a controlled manner. This can be done by a number of means, like electroless deposition or chemical functionalization as well as by sputtering and atomic layer deposition.[13−17] This is the reason why surface modification of nanopores and nanochannels has become an important object of study of a number of research groups.

On the other hand, electrostatic self-assembly of polyelectrolytes represents a method that has been used in the past few years to obtain smart and functional devices in a variety of confined geometries.[18] Even though promising applications of this supramolecular method have been shown (regarding its versatility and simplicity), the behavior of polyelectrolytes in confinement is not yet fully understood.[19−21]

Until now, the conformation of polyelectrolytes within nanochannels has been studied by means of gas-flow porometry and scanning electron microscopy. These investigations revealed that polyelectrolytes tend to form either nanowires or nanotubes for smaller and larger nanochannels diameters, respectively.[22,23] However, these experiments were performed in dry conditions, and consequently, the information about the conformation of the polymers cannot be extrapolated to nanofluidic experiments in which polymers are in a hydrated state. In this regard, theoretical modeling and fitting can be used to obtain information about the effect of the confinement of the polymers in aqueous environments. There are several examples in the literature about the advantages of theoretical approaches to understand the behavior of species under nanometric confinement.[24,25]

In the present work, we have modified the surface of a solid-state nanochannel with the polycation poly(allylamine hydrochloride) (PAH) and studied the concomitant changes in the nanopore surface charge as a function of the concentration of protons in solution. As a result, a pH-responsive nanofluidic device displaying a fully tunable and reversible ionic rectification was obtained and characterized. With regard to obtaining a complete physicochemical understanding of the system, experiments were accompanied by theoretical calculations based on the Poisson−Nernst−Planck (PNP) equations and Monte Carlo simulations (MC). To our knowledge, this is the first time that MC simulations have been applied to explain experimental results in nanofluidic systems modified with protonable species.

■ EXPERIMENTAL METHODS

Materials. Poly(allylamine hydrochloride) (PAH, M_w = 15 kDa) was purchased from Sigma-Aldrich and used as received. Single-ion-irradiated PET foils (Hostaphan RN 12, Hoechst) of 12 μm were irradiated at the linear accelerator UNILAC in GSI (Darmstadt, Germany, http://www.gsi.de) with swift heavy ions (Au) having an energy of 11.4 MeV per nucleon.

Chemical Etching. Two different etching procedures were utilized to obtain single asymmetric nanochannels from ion-tracked foils. On the one hand, conical geometries using 9 M sodium hydroxide as the etching solution and a mixture of 1 M formic acid and 1 M KCl as stopping solution while applying an electro-stopping field of 1 V were obtained. The applied potential has two purposes: (a) it increases the nanochannel's cone angle and (b) it allows the monitoring of the pore opening by observing the current flowing through the nanochannels.[26] On the other hand, to obtain more tapered geometries, a surfactant-assisted chemical etching was used.[27] The foils were first exposed to UV light for 35 h on one side only. The foil is subsequently inserted in an electrochemical cell, separating two cell compartments. The compartment facing the UV-pre-exposed polymer side was filled with etching solution (NaOH 6 M), while the other side was filled with the etching solution (NaOH 6 M) containing a surfactant (DOWFAX 2A1, 0.04%). The etching process was carried out at 60 °C for 6.5 min.

Many single-track nanochannels fabricated following the first etching procedure had to be discarded because they did not show ionic conductance. They were either "closed" or they closed shortly after measurements started and reopened only after higher transmembrane voltages were applied. Moreover, the ion current rectification factor of these nanochannels was much smaller than those obtained by the surfactant-assisted procedure. The surfactant-assisted procedure resulted in bullet-like (BL) nanochannels exhibiting high rectification factors. Therefore, all experimental results reported here were obtained using BL nanochannels.

Modification with Poly(allylamine hydrochloride). Single nanochannel membranes were modified by dip coating in an aqueous 10 mM poly(allylamine hydrochloride) solution (in monomer units) at a pH 6 for 2 h. The membranes were rinsed several times with distilled water and dried under ambient conditions.

Current−Voltage Measurements. Current−voltage curves were obtained using a potentiostat (Gamry Reference 600) with a four-electrode setup (working, working sense, reference and counter-electrode) to minimize the contribution from the processes occurring at the electrodes surfaces due to the voltage drop across the cell.[28] In this way, we are able to measure conductance variations arising from changes in the nanochannel. Both the working and counter-electrode were made of platinum, while the reference and working sense were commercial silver/silver chloride electrodes. A homemade conductivity cell was fabricated to avoid leakage currents; i.e., the compartments are connected by a single nanochannel. In all of the experiments the working electrode was placed at the tip of the nanochannel while the counter-electrode was placed at the base. A 0.1 M KCl solution was used as electrolyte. The same experimental setup has been used in all the experiments in order to unambiguously correlate $I-V$ plots with nanopore surface charges.

Rectification Factor. A rectification factor (f_{rec}), for quantifying the rectification efficiency, was defined. In all experiments, the definition for f_{rec} was

$$f_{rec} = \pm \left| \frac{I(1V \text{ or } -1V)}{I(-1V \text{ or } 1V)} \right| \quad (1)$$

Here, the current in the numerator is the largest current value corresponding to the high conductance state, while the

DOI: 10.1021/acs.jpcc.7b01639
J. Phys. Chem. C 2017, 121, 9070−9076

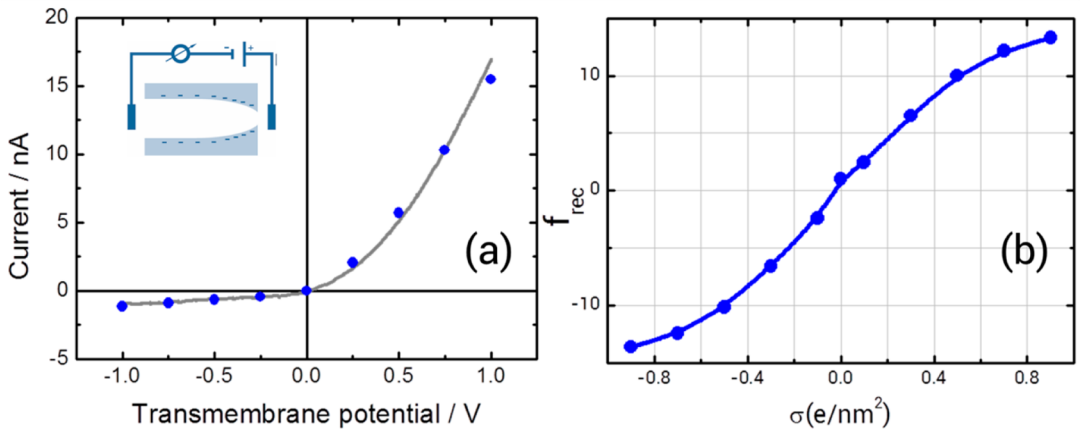

Figure 1. (a) Experimental results (gray line) and fitting with PNP model (blue dotted curve) for a bullet-like-etched PET nanochannel. Inset: Simplified scheme showing the electrode configuration. (b) Rectification factor versus surface charge density obtained from PNP theory for a bullet-like nanochannel. Tip diameter: 20 nm. Base diameter: 500 nm.

one in the denominator is the lowest current value corresponding to the low conductance state. Additionally, if the higher current corresponds to a positive voltage then the rectification factor is multiplied by −1 (Figure 1). This definition allows assigning a negative f_{rec} for the case of negative surface charges and positive f_{rec} for positive surface charges. This definition simplifies the interpretation of the experimental results in terms of surface charge.

Theoretical Methods. *Analytical Model.* In order to obtain information about the geometry and surface charge of the nanochannels after the modification with PAH, a theoretical modeling based on the one-dimensional PNP formalism was used.[29] BL nanochannels were modeled using parameters obtained either experimentally or from literature. Large opening (base) diameters of ∼500 nm were obtained from scanning electron microscopy imaging of multipore membranes (Figure S1). Other parameters such as the longitudinal profile and the native surface charge of the nanochannel were obtained from the literature. The surface charge density of the nanochannel was found to be between 1.5 and 1.7 |e|/nm^2. With these parameters, the best fits to the experimental $I-V$ curves yielded a small opening (tip) diameter of 20 nm.

The basic set of equations that were used to describe the transport through the nanochannels were the Nernst−Planck equation

$$\vec{J}_i = -D_i(\nabla c_i + z_i c_i \nabla \phi) \tag{2}$$

the Poisson equation

$$\nabla^2 \phi = -\frac{F^2}{\varepsilon RT} \sum_i z_i c_i \tag{3}$$

and the continuity equation

$$\nabla \vec{J} = 0 \tag{4}$$

where $\vec{J}_i$, D_i, z_i, and ε are the ionic flux, the diffusion coefficient, the ion charge, and the solution permittivity inside the channel, respectively.

Monte Carlo Simulations. MC simulations were performed in order to study the influence of the nanoconfinement on the acid−base equilibrium of a weak polyelectrolyte, i.e., PAH. The acid−base equilibrium has a strong influence on the experimental output measured as transmembrane currents.

For these studies, a simulation box containing a 5 nm diameter pore with a length of 20 nm was used. Both the monomers of PAH and the native carboxylic acid groups in the walls of the nanochannel were considered as weak electrolytes with the following acid−base equilibriums

$$-(NH_3^+)_n- \leftrightharpoons -(NH_2)_n- + nH^+$$

$$pK_a = 10.4 \text{ (monomers in the polymer chain)}$$

$$R{-}COOH \leftrightharpoons R{-}COO^- + H^+$$

$$pK_a = 3.5 \text{ (charges on the pore walls)}$$

The acidic behavior was investigated in a grand canonical ensemble. To perform the simulations, a monomer was randomly chosen and an attempt was made to switch its charge state. The free energy change, ΔE, governing the success of the attempt, can be described in terms of two major contributions: the change in the Coulombic interactions between monomers, cations and anions, ΔE_{total}, and the free energy change corresponding to the acid−base reaction of an isolated monomer[30,31]

$$\Delta E = \Delta E_{total} \pm k_B T \log(pH - pK_i) \tag{5}$$

where pH is the pH of the system and pK_i is the intrinsic pK_a of the monomer or the carboxylic groups on the pore walls. The plus sign in the equation is used when the monomer is protonated and the minus sign when it is deprotonated.

■ RESULTS AND DISCUSSION

Asymmetric nanochannels display the ability to rectify ionic current passing through them as a function of the sign and magnitude of the surface charges exposed on their walls.[32] This occurs, in principle, because charged nanochannels are highly selective to ionic species of opposite sign of the surface.[33] However, the mechanism underlying the rectification of ionic currents is a more complex phenomenon. We have recently shown that the transport number of cations in a conically etched PET nanochannel, that bears negative surface charges after etching, is close to 0.95 at negative voltages (low conductance state) but close to 0.5 at positive voltages (high conductance states) meaning that the emergence of rectification is due to a loss of the selectivity at positive potentials

DOI: 10.1021/acs.jpcc.7b01639
J. Phys. Chem. C 2017, 121, 9070−9076

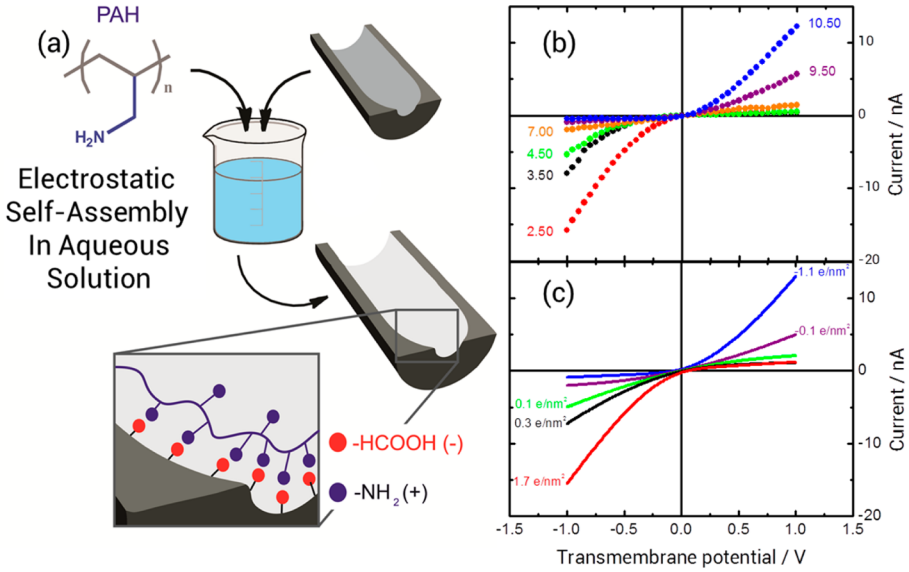

Figure 2. (a) Scheme showing the modification of the nanochannel with PAH and the ionizable groups in the surface. (b) Experimental curves of the modified nanochannel under different pH conditions (c). Theoretical curves of the modified nanochannel at different surface charges.

allowing both anions and cations to contribute to the transport of current.[34]

The current−voltage measurements of the nanochannel without any further modification correspond to a negatively charged surface (Figure 1a). Once the PNP modeling was performed, an excellent agreement between experimental and theoretical results was observed (Figure 1a). The PNP theory correlates the current−voltage characteristics (i.e., the rectification efficiency) of a given nanochannel with the surface charge. For a fixed geometry, we observed a monotonic increase in the rectification factor upon increasing the surface charge (Figure 1b), which confirms that a functional molecule that can finely modify its state of charge can consequently transduce these changes into the direction and magnitude of the ionic transport.

The native negative charge of the nanochannels stems from the chemical nature of PET. The hydrolysis performed during the etching of the nanochannel leads to the appearance of carboxylate groups on the surface. These negative groups were used for the electrostatic assembly of PAH, a polycation that strongly interacts with negative species (Figure 2).

After PAH modification, $I-V$ curves at different pH values were measured. Figure 2 shows the $I-V$ curves for a PAH-modified nanochannel in 0.1 M KCl measured under different conditions and the simulated curves using the PNP model. The change in the shape of the $I-V$ curves follows a continuous trend that can be clearly observed in the f_{rec} vs pH plots (Figure 3). In the pH range of 4−8 a reversion in the rectification direction, i.e., reversion of f_{rec}, sign was observed. This result was reproduced on different nanochannels.

The behavior of the rectification factor with pH showed an extended low rectification region between pH 5 and 8. The PNP model was then used to correlate rectification factors with the surface charge density on the nanochannel walls, finding that this region exhibits a net charge close to zero. For this reason, we chose to refer to this region as the *isoelectric region* (IR) (Figure 3). In order to quantify the variation in magnitude and sign of the surface charge with pH, the charge was calculated for each experimental curve measured under different pH conditions (Figure 3b).

The maximum value obtained for a nanochannel modified with PAH at low pH was 1.7|e|/nm^2, which is close to the native anionic charge density of the nanochannel. On the other hand, the maximum negative surface charge obtained after the modification at high pH was −1.1|e|/nm^2, which is slightly lower than the initial surface charge of the nanochannel. This difference can be explained taking into account that negative charges can only arise from the PET surface underneath the PAH layer. After the modification, at high pH, the PAH starts to deprotonate, until the net charge becomes negative due to the ionized carboxylate groups present on the PET foil. The fact that this net negative charge is lower than the initial value can be explained by considering that some groups of the PAH must remain protonated even at high pH. This was indeed confirmed by MC simulations. They showed that the PAH remains slightly protonated (charged) even at very high pH values (Figure 3). Figure 3c shows 10% of the PAH amine groups is still protonated at pH values as high as 12. Furthermore, considering the electrostatic charges stemming from the protonated polymer and the surface it was possible to calculate the contributions to the surface charge arising from the adsorbed polymer and the nanochannel surface (Figure 3b).

From these results, it can be seen that within the IR both the native nanochannel carboxylic groups and the adsorbed polycation remain in a highly charged state, strongly interacting with each other.

The isoelectric region was also studied using MC simulations after calculating the net charge inside the channel (Figure 3b, red curve). From MC simulations we concluded that the region between pH 5 and 8 (IR) can be interpreted as a region where there is significant negative charge from carboxylate groups that are highly deprotonated (Figure 3c, green curve) and positive charges from the PAH amine groups which, in turn, are highly protonated (Figure 3c, blue curve). Even though both groups are strongly charged, local electrostatic neutralization occurs and the net charge is zero.

Previous works have theoretically and experimentally shown that the apparent pK_a of a weak polyelectrolyte shifts by increasing the confinement. For the case of polybases like the PAH a shift in the pK_a toward higher values is expected due to

DOI: 10.1021/acs.jpcc.7b01639
J. Phys. Chem. C 2017, 121, 9070−9076

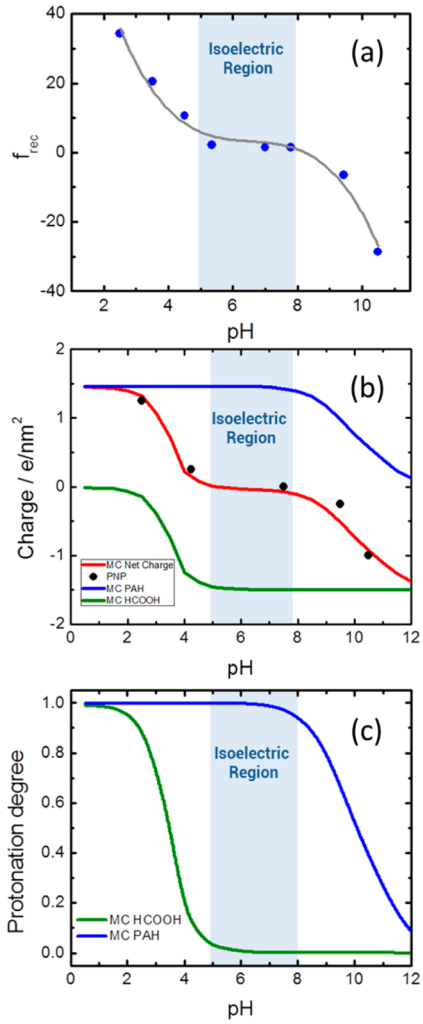

Figure 3. (a) Rectification factor as a function of pH calculated using eq 1. (b) Surface charge density versus pH as derived from (i) the fitting of the experimental $I-V$ curves using the PNP formalism, (ii) MC simulations, and (iii) the fitting between experimental and PNP $I-V$ curves. (c) Protonation degree vs pH obtained from MC simulations.

loss of degrees of freedom.[35−38] These previous observations are in agreement with our results. It is important to note that both PNP and MC methods are in excellent agreement with each other and also with the experimental results.

Even though the PNP model allowed us to accurately fit experimental results, it evidenced difficulties at extreme pH values. The maximum rectification factor obtained for the simulations was 15 while the experimental maximum values were ∼30. The difference between experimental and theoretical values stems mainly from ionic currents in the lower conductivity state. For the calculation of rectification factors, small differences in these current values may produce large variations in the f_{rec} values (eq 1). Similar differences have been reported previously.[39,27,29] One of the causes of these discrepancies could be an inhomogeneity on the surface charge that might exist in real nanochannels and that is not taken into account in the theory.

Also, it is important to take into account that the PNP model assumes that the charge is one-dimensional while in our experiments the charge is expected to have a tridimensional distribution due to the presence of the adsorbed polymer.[40] In this regard, it was theoretically shown that in nanochannels modified with polyelectrolytes with a degree of polymerization of 40 rectification factors up to 42 can be reached.[39] Further research needs to be performed in order to address these questions.

Another important issue to address was the system's reversibility, i.e., the capacity of exposing the system to successive cycles of extreme pH values without losing its responsiveness. It has been shown that in planar substrates, the application of extreme pH and ionic strength conditions can lead to the disassembly of polyelectrolyte multilayers, especially when constituted of weak polyelectrolytes.[41−43] This feature has been used for drug delivery by controlling the disassembly of multilayered structures containing specific molecules inside. However, in the case of nanofluidic applications pH-induced disassembly of the functional layer is undesired. Testing the reversibility by changing the pH of the electrolyte solution successively between 2.5 and 10.5 confirmed the robustness of the modification procedure (Figure 4).

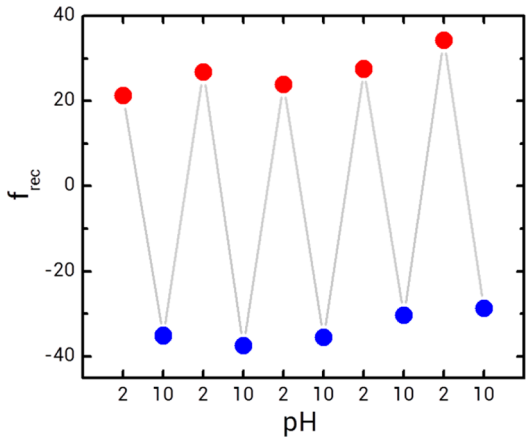

Figure 4. Reversibility test: The frec were calculated from experiments measured at extreme pH successively. A high reversibility is observed.

High rectification efficiencies were obtained for each cycle. Normal f_{rec} for surface modified nanochannels are around ∼5. We obtained f_{rec} of ∼30 which are comparable with the ones obtained for nanochannels modified with densely charged polymer brushes that required more complex synthetic protocols. The fact that the PAH remains inside the nanochannel even upon the exposure to extreme pH can be explained considering the protonation degree of the polyelectrolyte obtained from MC simulations (Figure 3). These results reveal that at *low pH* PAH is fully *protonated,* while the carboxylate groups are not. On the other hand, at *high pH,* the carboxylate groups are fully *deprotonated* while the PAH is not. However, even at extreme pH values such as 2 or 10 there are carboxylate and amine groups that still remain unprotonated or protonated, respectively, allowing electrostatic interactions to restrain the PAH from leaving the channel.

The functional features of this experimental system closely resemble those observed in biological KcsA ion channels. This family of ionic channel proteins shows pH and voltage-controlled ion gating.[44] As can be seen in Figure 5, there is a pH-induced *on−off* switch at a fixed voltage. This behavior is then reversed by applying the opposite voltage. This means that by applying different combinations of pH and voltage the selective transport of ionic species can be fully regulated.

DOI: 10.1021/acs.jpcc.7b01639
J. Phys. Chem. C 2017, 121, 9070−9076

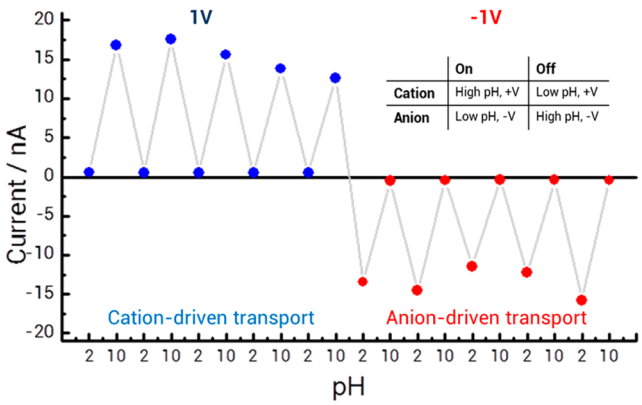

Figure 5. Ionic currents measured at different pH and transmembrane voltages. These results show the gating capacity of a PAH-modified nanochannel. Different combinations of pH and voltage allow control of the selective passage of ions through the nanochannel.

■ CONCLUSIONS

We demonstrated a simple and highly effective way to control the ionic transport properties of asymmetric nanochannels in the presence of different proton concentrations in solution. The procedure consisted of coating a hydrolyzed nanochannel-containing foil with a weak polycation, poly(allylamine hydrochloride). Poisson−Nernst−Planck equations were used to calculate the surface charge densities under different pH conditions, and Monte Carlo simulations were performed to study the relationship between the protonation degrees of the PAH layer and the ionizable surface groups on the nanochannel wall, and the solution pH. We showed that the ionic transport properties of the nanochannel are governed by a delicate interplay between the negatively charged carboxylic groups of the nanochannel walls and the positively charged primary amines on the PAH layer. It is shown that the shift in the protonation degree of amino and carboxyl groups prevents the removal of the PAH layer from the nanochannel due to presence of residual charges, even in the case of extreme pH conditions. Furthermore, the capabilities of the system to act as a biomimetic pH- and voltage-controlled ionic gate were demonstrated. Taking into account that simple derivatization of pendant amino groups of the polyallylamine layer with different chemical groups can endow nanochannels with predefined responsiveness or multiple functions, we believe that these results can inspire further research toward advanced design of nanofluidic devices.

■ ASSOCIATED CONTENT

Supporting Information

The Supporting Information is available free of charge on the ACS Publications website at DOI: 10.1021/acs.jpcc.7b01639.

SEM images of multitrack foils used for performing the PNP calculations (PDF)

■ AUTHOR INFORMATION

Corresponding Authors

*E-mail: gperezmitta@inifta.unlp.edu.ar. Web: https://softmatter.quimica.unlp.edu.ar and https://www.facebook.com/SoftMatterLaboratory/.

*E-mail: azzaroni@inifta.unlp.edu.ar. Web: https://softmatter.quimica.unlp.edu.ar and https://www.facebook.com/SoftMatterLaboratory/.

ORCID

Omar Azzaroni: 0000-0002-5098-0612

Notes

The authors declare no competing financial interest.

■ ACKNOWLEDGMENTS

We acknowledge financial support from ANPCyT (PICT 2010-2554, PICT-2013-0905 and PPL 2011-003) and from the Deutsche Forschungsgemeinschaft (DFG-FOR 1583). M.E.T.-M and C.T. acknowledge support by the LOEWE project iNAPO funded by the Hessen State Ministry of Higher Education, Research and Arts. G.P.-M. and F.M.G. acknowledge CONICET for a doctoral fellowship. A.A. and O.A. are staff members of CONICET.

■ REFERENCES

(1) Hou, X.; Zhang, H.; Jiang, L. Building Bio-Inspired Artificial Functional Nanochannels: From Symmetric to Asymmetric Modification. *Angew. Chem., Int. Ed.* **2012**, *51*, 5296−5307.

(2) Venkatesan, B. M.; Bashir, R. Nanopore Sensors for Nucleic Acid Analysis. *Nat. Nanotechnol.* **2011**, *6*, 615−624.

(3) Hou, X. Smart Gating Multi-Scale Pore/Channel-Based Membranes. *Adv. Mater.* **2016**, *28*, 7049−7064.

(4) Kong, Y.; Fan, X.; Zhang, M. H.; Hou, X.; Liu, Z. Y.; Zhai, J.; Jiang, L. Nanofluidic Diode Based on Branched Alumina Nanochannels with Tunable Ionic Rectification. *ACS Appl. Mater. Interfaces* **2013**, *5*, 7931−7936.

(5) Siwy, Z.; Apel, P. Y.; Baur, D.; Dobrev, D. D.; Korchev, Y. E.; Neumann, R.; Spohr, R.; Trautmann, C.; Voss, K.-O. Preparation of Synthetic Nanopores with Transport Properties Analogous to Biological Channels. *Surf. Sci.* **2003**, *532*, 1061−1066.

(6) Yameen, B.; Ali, M.; Neumann, R.; Ensinger, W.; Knoll, W.; Azzaroni, O. Ionic Transport Through Single Solid-State Nanopores Controlled with Thermally Nanoactuated Macromolecular Gates. *Small* **2009**, *5*, 1287−1291.

(7) Zhang, H.; Hou, X.; Yang, Z.; Yan, D.; Li, L.; Tian, Y.; Wang, H.; Jiang, L. Bio-inspired Smart Single Asymmetric Hourglass Nanochannels for Continuous Shape and Ion Transport Control. *Small* **2015**, *11*, 786−791.

(8) Hou, X.; Guo, W.; Jiang, L. Biomimetic Smart Nanopores and Nanochannels. *Chem. Soc. Rev.* **2011**, *40*, 2385−2401.

(9) Kocer, A.; Tauk, L.; Dejardin, P. Nanopore sensors: From Hybrid to Abiotic Systems. *Biosens. Bioelectron.* **2012**, *38*, 1−10.

(10) Fleischer, R. L.; Price, P. B.; Walker, R. M. *Nuclear Tracks in Solids: Principles and Applications*; University of California Press: Berkeley, 1975.

(11) Siwy, Z.; Apel, P. Y.; Dobrev, D.; Neumann, R.; Spohr, R.; Trautmann, C.; Voss, K.-O. Ion Transport Through Asymmetric Nanopores Prepared by Ion Track Etching. *Nucl. Instrum. Methods Phys. Res., Sect. B* **2003**, *208*, 143−148.

(12) Siwy, Z.; Dobrev, D.; Neumann, R.; Trautmann, C.; Voss, K.-O. Electro-Responsive Asymmetric Nanopores in Polyimide with Stable Ion-Current Signal. *Appl. Phys. A: Mater. Sci. Process.* **2003**, *76*, 781−785.

(13) Martin, C. R. Membrane-Based Synthesis of Nanomaterials. *Chem. Mater.* **1996**, *8*, 1739−1746.

(14) Yameen, B.; Ali, M.; Neumann, R.; Ensinger, W.; Knoll, W.; Azzaroni, O. Synthetic Proton-Gated Ion Channels via Single Solid-State Nanochannels Modified with Responsive Polymer Brushes. *Nano Lett.* **2009**, *9*, 2788−2793.

(15) Zhang, H.; Hou, X.; Hou, J.; Zeng, L.; Tian, Y.; Li, L.; Jiang, L. Synthetic Asymmetric-Shaped Nanodevices with Symmetric pH-Gating Characteristics. *Adv. Funct. Mater.* **2015**, *25*, 1102−1110.

DOI: 10.1021/acs.jpcc.7b01639
J. Phys. Chem. C 2017, 121, 9070−9076

(16) Hou, X.; Liu, Y.; Dong, H.; Yang, F.; Li, L.; Jiang, L. A pH-Gating Ionic Transport Nanodevice: Asymmetric Chemical Modification of Single Nanochannels. *Adv. Mater.* **2010**, *22*, 2440−2443.
(17) Spende, A.; Sobel, N.; Lukas, M.; Zierold, R.; Riedl, J. C.; Gura, L.; Schubert, I.; Montero Moreno, J. M.; Nielsch, K.; Stühn, B. TiO2, SiO2, and Al2O3 Coated Nanopores and Nanotubes Produced by ALD in Etched Ion-Track Membranes for Transport Measurements. *Nanotechnology* **2015**, *26*, 335301−335312.
(18) Azzaroni, O.; Lau, K. H. A. Layer-by-Layer Assemblies in Nanoporous Templates: Nano-Organized Design and Applications of Soft Nanotechnology. *Soft Matter* **2011**, *7*, 8709−8724.
(19) Lee, D.; Nolte, A. J.; Kunz, A. L.; Rubner, M. J.; Cohen, R. E. PH-Induced Hysteretic Gating of Track-Etched Polycarbonate Membranes: Swelling/Deswelling Behavior of Polyelectrolyte Multilayers in Confined Geometry. *J. Am. Chem. Soc.* **2006**, *128*, 8521−8529.
(20) Ali, M.; Yameen, B.; Neumann, R.; Ensinger, W.; Knoll, W.; Azzaroni, O. Biosensing and Supramolecular Bioconjugation in Single Conical Polymer Nanochannels. Facile Incorporation of Biorecognition Elements into Nanoconfined Geometries. *J. Am. Chem. Soc.* **2008**, *130*, 16351−16357.
(21) Ali, M.; Yameen, B.; Cervera, J.; Ramírez, P.; Neumann, R.; Ensinger, W.; Knoll, W.; Azzaroni, O. Layer-by-Layer Assembly of Polyelectrolytes into Ionic Current Rectifying Solid-State Nanopores: Insights from Theory and Experiment. *J. Am. Chem. Soc.* **2010**, *132*, 8338−8348.
(22) Roy, C. J.; Dupont-Gillain, C.; Demoustier-Champagne, C.; Jonas, A. M.; Landoulsi, J. Growth Mechanism of Confined Polyelectrolyte Multilayers in Nanoporous Templates. *Langmuir* **2010**, *26*, 3350−3355.
(23) Alem, H.; Blondeau, F.; Glinel, K.; Demoustier-Champagne, S.; Jonas, A. M. Layer-by-Layer Assembly of Polyelectrolytes in Nanopores. *Macromolecules* **2007**, *40*, 3366−3372.
(24) Cervera, J.; Schiedt, B.; Ramırez, P. A. Poisson/Nernst-Planck Model for Ionic Transport Through Synthetic Conical Nanopores. *Europhys. Lett.* **2005**, *71*, 35−41.
(25) Sparreboom, W.; Van den Berg, A.; Eijkel, J. C. T. Transport in Nanofluidic Systems: A Review of Theory and Applications. *New J. Phys.* **2010**, *12*, 015004−015027.
(26) Siwy, Z.; Fulinski, A. A Nanodevice for Rectification and Pumping ions. *Am. J. Phys.* **2004**, *72*, 567−574.
(27) Apel, P. Y.; Blonskaya, I. V.; Levkovich, N. V.; Orelovich, O. L. Asymmetric Track Membranes: Relationship Between Nanopore Geometry and Ionic Conductivity. *Pet. Chem.* **2011**, *51*, 555−567.
(28) Application note: http://www.gamry.com/application-notes/electrodes-cells/two-three-and-four-electrode-experiments/.
(29) Cervera, J.; Schiedt, B.; Neumann, R.; Mafé, S.; Ramírez, P. Ionic, Ionic Conduction, Rectification, and Selectivity in Single Conical Nanopores. *J. Chem. Phys.* **2006**, *124*, 104706.
(30) Albesa, A. G.; Rafti, M.; Vicente, J. L. Trivalent Cations Switch the Selectivity in Nanopores. *J. Mol. Model.* **2013**, *19*, 2183−2188.
(31) Barr, S. A.; Panagiotopoulos, A. Z. Conformational Transitions of Weak Polyacids Grafted to Nanoparticles. *J. Chem. Phys.* **2012**, *137*, 144704.
(32) Harrell, C. C.; Siwy, Z. S.; Martin, C. R. Conical Nanopore Membranes: Controlling the Nanopore Shape. *Small* **2006**, *2*, 194−198.
(33) Siwy, Z. S.; Martin, C. R. Tuning Ion Current Rectification in Synthetic Nanotubes. *Lect. Notes Phys.* **2007**, *711*, 349−365.
(34) Pérez-Mitta, G.; Albesa, A. G.; Toimil-Molares, M. E.; Trautmann, C.; Azzaroni, O. The Influence of Divalent Anions on the Rectification Properties of Nanofluidic Diodes: Insights from Experiments and Theoretical Simulations. *ChemPhysChem* **2016**, *17*, 2718−2725.
(35) Longo, G. S.; Olvera de La Cruz, M.; Szleifer, I. Molecular Theory of Weak Polyelectrolyte Gels: The Role of pH and Salt Concentration. *Macromolecules* **2011**, *44*, 147−158.
(36) Choi, J.; Rubner, M. F. Influence of The Degree of Ionization on Weak Polyelectrolyte Multilayer Assembly. *Macromolecules* **2005**, *38*, 116−124.
(37) Itano, K.; Choi, J.; Rubner, M. F. Mechanism of the pH-Induced Discontinuous Swelling/Deswelling Transitions of Poly(allylamine hydrochloride)-Containing Polyelectrolyte Multilayer Films. *Macromolecules* **2005**, *38*, 3450−3460.
(38) Petrov, A. I.; Antipov, A. A.; Sukhorukov, G. B. Base−Acid Equilibria in Polyelectrolyte Systems: From Weak Polyelectrolytes to Interpolyelectrolyte Complexes and Multilayered Polyelectrolyte Shells. *Macromolecules* **2003**, *36*, 10079−10086.
(39) Tagliazucchi, M.; Rabin, Y.; Szleifer, I. Transport Rectification in Nanopores with Outer Membranes Modified with Surface Charges and Polyelectrolytes. *ACS Nano* **2013**, *7*, 9085−9097.
(40) Tagliazucchi, M.; Azzaroni, O.; Szleifer, I. Responsive Polymers End-Tethered in Solid-State Nanochannels: When Nanoconfinement Really Matters. *J. Am. Chem. Soc.* **2010**, *132*, 12404−12411.
(41) Lynn, D. M. Peeling Back the Layers: Controlled Erosion and Triggered Disassembly of Multilayered Polyelectrolyte Thin Films. *Adv. Mater.* **2007**, *19*, 4118−4130.
(42) Sukhishvili, S. A.; Granick, S. Layered, Erasable, Ultrathin Polymer Films. *J. Am. Chem. Soc.* **2000**, *122*, 9550−9551.
(43) Dubas, S. T.; Farhat, T. R.; Schlenoff, J. B. Multiple Membranes from "True" Polyelectrolyte Multilayers. *J. Am. Chem. Soc.* **2001**, *123*, 5368−5369.
(44) Hirano, M.; Onishi, Y.; Yanagida, T.; Ide, T. Role of the KcsA Channel Cytoplasmic Domain in pH-Dependent Gating. *Biophys. J.* **2011**, *101*, 2157−2162.

DOI: 10.1021/acs.jpcc.7b01639
J. Phys. Chem. C 2017, 121, 9070−9076